

## Network Rigidity in GeSe<sub>2</sub> Glass at High Pressure

Sytle M. Antao,<sup>1,\*</sup> Chris J. Benmore,<sup>1</sup> Baosheng Li,<sup>2</sup> Liping Wang,<sup>2</sup> Evgeny Bychkov,<sup>3</sup> and John B. Parise<sup>2</sup>

<sup>1</sup>Advanced Photon Source, Argonne National Laboratory, Argonne, Illinois 60439, USA

<sup>2</sup>Mineral Physics Institute and Department of Geosciences, Stony Brook University, Stony Brook, New York 11794-2100, USA

<sup>3</sup>LPCA, UMR 8101 CNRS, Université du Littoral, 59140 Dunkerque, France

(Received 12 September 2007; published 18 March 2008)

Acoustic measurements using synchrotron radiation have been performed on glassy GeSe<sub>2</sub> up to pressures of 9.6 GPa. A minimum observed in the shear-wave velocity, associated anomalous behavior in Poisson's ratio, and discontinuities in elastic moduli at 4 GPa are indicative of a gradual structural transition in the glass. This is attributed to a network rigidity minimum originating from a competition between two densification mechanisms. At pressures up to 3 GPa, a conversion from edge- to corner-sharing tetrahedra results in a more flexible network. This is contrasted by a gradual increase in coordination number with pressure, which leads to an overall stiffening of the glass.

DOI: 10.1103/PhysRevLett.100.115501

PACS numbers: 61.43.Fs, 61.05.cp

Gradual structural transitions in glasses, which occur via continuous changes in density, are inherently difficult to identify due to their disordered nature. Such transitions may often be hidden in glass diffraction data although they are important throughout the field of materials science. Acoustic techniques, however, can be applied to a variety of materials to identify phase transitions (especially second order or higher) and obtain elastic properties of solid bulk materials. While the measured compressional velocities can be linked to density changes in the glass, shear waves in glasses provide an insight into network rigidity and this is demonstrated most dramatically with the application of pressure [1]. State-of-the-art ultrasonic interferometry offers direct measurements of sound velocities, and hence, elastic properties (Fig. 1). For example, recent results on magnesioferrite spinel show that order-disorder and magnetic transitions have a marked effect on velocities [2]. Large-volume multianvil apparatus, with simultaneous pressure generation and ultrasonic measurements, have been used to observe the effect on shear (*S*) and compressional (*P*) wave velocities during the densification process in amorphous GeSe<sub>2</sub>. While *S* waves are not readily transmitted through a liquid, they are sensitive to network rigidity in a solid glass (or frozen liquid).

Binary Ge-Se glasses have long been the basis for network rigidity theories because they form homogenous bulk glasses over a wide compositional range with a continuous variation in average coordination number [3–7]. Mean-field theory predicts an onset of network rigidity as the coordination number *n* for *n* > 2.4 reaches a fully polymerized network at *n* = 2.67 for GeSe<sub>2</sub> [8]. At the GeSe<sub>2</sub> composition the glass has a rigid structure composed primarily of GeSe<sub>4</sub> tetrahedra. Neutron diffraction results have shown that 34% of the tetrahedra are in edge-sharing configurations and the rest are corner shared, with a significant number of “wrong” or homopolar bonds present [9] (Fig. 1). These tetrahedra are arranged in a distribution of ring sizes containing predominantly 3, 6, 7, and 8 Ge atoms [10–13]. However, the observed trends of

intermediate-range order mainly due to cation-cation correlations do not correlate with predicted rigidity percolation limits. Consequently, it has been suggested that network rigidity and static intermediate-range order structural information obtained from diffraction experiments are not closely related in the case of binary selenide glasses [14]. In this Letter, we present evidence of a network rigidity minimum in GeSe<sub>2</sub> glass at a pressure of 4 GPa, based on *in situ* acoustic measurements, demonstrating that network transitions in glasses may occur even with a continuous variation in density.

The GeSe<sub>2</sub> sample was synthesized from high-purity elements at the Université du Littoral, France, and additional details are given elsewhere [15]. The initial density of the sample was  $\sim 4.2 \text{ g cm}^{-3}$  and the density of the recovered sample after the high-pressure ultrasonic study was  $\sim 4.4 \text{ g cm}^{-3}$ . Ultrasonic measurements at pressure were performed using a DIA-type, large-volume apparatus (SAM85) in conjunction with *in situ* energy-dispersive x-ray techniques, at the X17B2 beam line of the National Synchrotron Light Source at Brookhaven National Laboratory. Details of this experimental setup

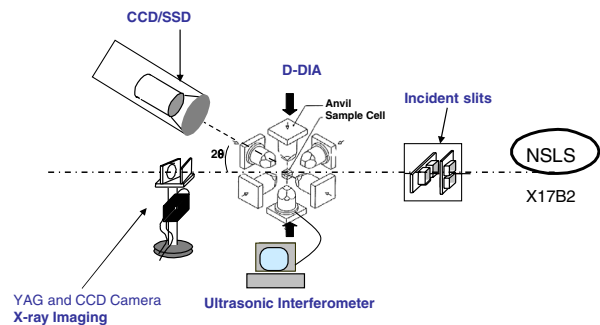


FIG. 1 (color online). Schematic experimental setup at X17B2, NSLS, for simultaneous pressure-volume-temperature equation-of-state and sound-velocity measurement. The thick arrows indicate the top and bottom anvils that can be advanced or retracted to minimize stress.

have been described elsewhere [16]. The cell assembly was  $6.2 \times 6.2 \times 6.2 \text{ mm}^3$ , made of a mixture of boron and epoxy resin as the pressure medium. A layer of NaCl was loaded into the cell, which provided a pseudohydrostatic environment as well as a pressure calibrant. X-ray diffraction data of the sample and NaCl were obtained in the energy-dispersive mode with a solid-state Ge detector. The incident beam was collimated to 0.2 mm by 0.1 mm and the diffraction angle was set at  $2\theta = 6.5^\circ$ . The measured cell parameter of NaCl was used to determine the cell pressure using Decker's equation of state [17]. The NaCl peaks were also monitored for stress and the top and bottom anvils of the DIA apparatus were either advanced or retracted in order to minimize stress and prevent the brittle  $\text{GeSe}_2$  sample from cracking. The pressure was gradually increased to about 9 GPa and x-ray and ultrasonic data were continuously collected. No evidence of devitrification was observed during the experiment.

Two-way travel times of ultrasonic waves through the specimen were determined using a transfer-function method that has recently been developed [16,18]. With this new system, the travel times were measured using the pulse echo overlap method. Dual-mode  $\text{LiNbO}_3$  transducers ( $10^\circ$  rotated  $Y$  cut) were used to generate and receive ultrasonic signals; these transducers generate both longitudinal ( $P$ ) and transverse ( $S$ ) acoustic signals simultaneously with unspecified polarization of the transverse signal [19,20]. The acoustic travel time, measured at high pressure, consists of a pathway through the tungsten-carbide cube, polycrystalline  $\text{Al}_2\text{O}_3$  (Coors998) buffer rod, sample, and NaCl. Thin gold foils ( $1 \mu\text{m}$  thick) at both ends of the sample were used to improve the acoustic coupling between the interfaces. The round-trip travel time for the  $P$  wave was averaged from 45 to 55 MHz and for the  $S$  wave from 35 to 45 MHz. The errors in travel times are about 0.4 ns for the  $S$  wave and 0.2 ns for the  $P$  wave.

The sample length is monitored (not inferred) continuously using the radiographic technique throughout the course of the high-pressure experiment and used to calculate sound velocities directly from measured travel times. An enlarged x-ray beam passes through the gaps between the anvils and the cell assembly and illuminates a fluorescent yttrium aluminum garnet (YAG) crystal (Fig. 2). The visible light generated by the YAG crystal is reflected by a mirror into the CCD camera, where an image of the cell is captured [21]. The contrasting intensities at different regions of the image are caused by the differences in the x-ray absorption of all materials in the cell assembly. A sequence of x-ray images was recorded during the course of collecting ultrasonic data at high pressure. The final image taken at ambient conditions when the press was opened at the end of the experiment, and the measured length of the recovered sample, provide the conversion factor between the actual specimen dimension and images [16,19]. The precision of this direct measurement of sample length was reported to be 0.2%–0.4% [16]. The compressional ( $V_P$ ) and shear ( $V_S$ ) velocities were calculated

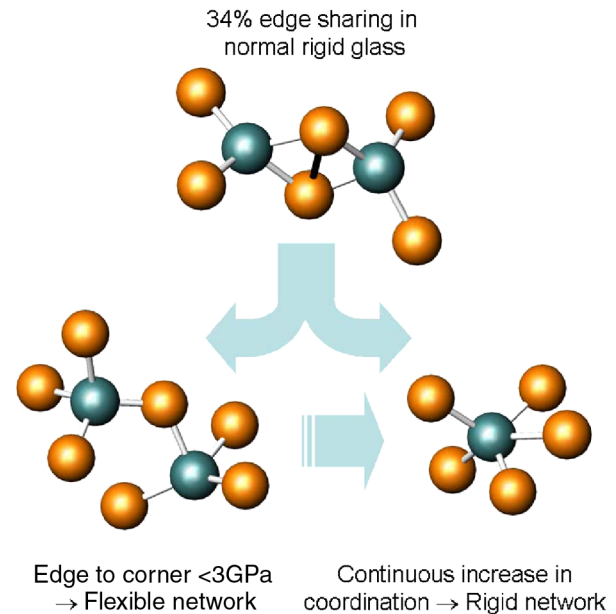


FIG. 2 (color online). Dominant densification mechanisms in  $\text{GeSe}_2$  glass at high pressure.

with measured travel times and sample lengths ( $l$ ) at the different pressure using the general relationship  $V_{(P,S)} = l/t_{(P,S)}$ . An error propagation analysis, based on the uncertainties in the measured length and travel time, indicates that the uncertainties in velocities are less than 0.6%.

Data on the elastic properties of Ge-Se glasses are available [22–25]. However, for the  $\text{GeSe}_2$  composition only an estimation of the velocities exists; the velocities for  $\text{GeSe}_2$  at 1 atm were extrapolated to  $V_S = 1.62$  and  $V_P = 2.8 \text{ km/s}$  [25]. In this study the velocities at 1 GPa are  $V_S = 1.76$  and  $V_P = 2.52 \text{ km/s}$ . The  $V_P$  increases gradually with pressure while the  $V_S$  anomalously decreases up to 4.5 GPa, and then increases to 9.5 GPa [Figs. 3(a) and 3(b)].  $\text{SiO}_2$  glasses were found to exhibit anomalous minima in both  $P$ - and  $S$ -wave velocities around 3 GPa [26–30]. However, in this study the minimum was observed only for the  $S$  wave at about 4 GPa. We attribute this anomaly to changes in the structure of the glass. Prasad *et al.* [31] observed changes in ambient resistivity for  $\text{Ge}_x\text{Se}_{100-x}$  glasses with increasing pressure. These glasses with composition  $x \geq 15$  exhibit an initial positive pressure coefficient of electrical resistivity, followed by a continuous decrease, a behavior typical for glasses with tetrahedral local structures [32].

Equation-of-state measurements show a gradual increase in the density of  $\text{GeSe}_2$  glass under pressure, up to 33% at 8.5 GPa [15], which is consistent with the steady increase in  $P$ -wave velocity with pressure. Similarly, *ab initio* molecular dynamics simulations predict gradual structural changes in  $\text{GeSe}_2$  glass with pressure, accompanied by a reduction in chemical disorder up to 13 GPa [5]. Raman studies have indicated that a conversion of edge- to corner-sharing tetrahedra is the dominant densifi-

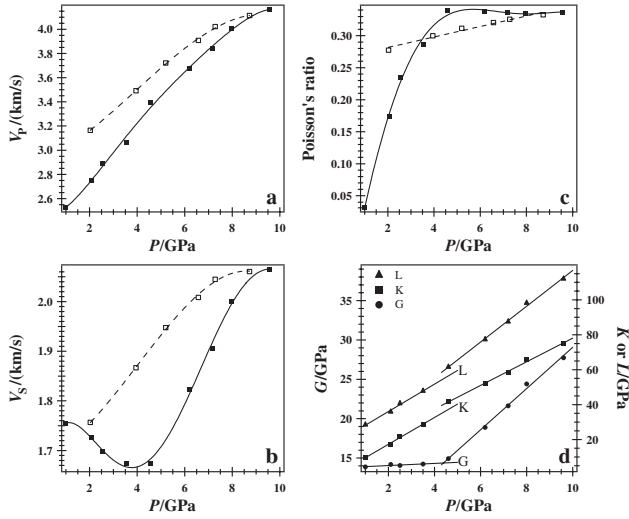


FIG. 3. Variations with pressure. (a)  $V_p$ , (b)  $V_s$ , (c) Poisson's ratio, and (d) elastic moduli. Solid symbols are data on pressurization and open symbols are data on depressurization. Lines in (a)–(c) are polynomial fits as guides to the eye. In (d), linear trend lines are fit to the data above and below 4 GPa (shear or rigidity modulus  $G = \rho V_s^2$ ; bulk modulus  $K = \rho(V_p^2 - \frac{4}{3}V_s^2)$ ; longitudinal modulus  $L = \rho V_p^2$ ).

cation mechanism up to 3 GPa, beyond which the edge- to corner-sharing ratio remains constant (Fig. 2) [33]. High-energy x-ray diffraction experiments up to 9.6 GPa have shown that a gradual increase in average coordination number occurs with increasing pressure, and this process is expected to dominate at pressure  $>4$  GPa. Furthermore, the conversion from tetrahedra to higher-order polyhedra are accompanied by an elongation of the mean Ge-Se bond length, together with an increase in extended-range order [34].

The minimum observed in the  $S$ -wave velocity with pressure for GeSe<sub>2</sub> glass at 4 GPa is interpreted as a result of competition between these two densification mechanisms. Namely, at low pressure  $<3$  GPa the network becomes more flexible as the connectivity decreases due to the breakup of cross-linking elements [8]. Above 4 GPa the covalently bonded network progressively stiffens as its mean coordination number increases [35]. On depressurization, both velocities decrease irreversibly to ambient pressure due to permanent densification, and no minima is observed in  $V_s$ . Isotopic neutron and high-energy x-ray diffraction data on GeSe<sub>2</sub> glasses recovered from 10 GPa show that on depressurization the Ge-Se bond length remains elongated and, although the compacted samples revert back to tetrahedral coordination, they remain highly distorted [15].

Poisson's ratio  $\sigma$  is obtained directly from the measured velocities by the equation

$$\sigma = \frac{V_p^2 - 2V_s^2}{2(V_p^2 - V_s^2)}.$$

The variation of Poisson's ratio is displayed in Fig. 3(c). On pressurization,  $\sigma$  increases monotonically from 0.03 at 1 GPa to 0.34 at 4.5 GPa, beyond which it becomes nearly pressure independent. A similar trend was observed for SiO<sub>2</sub> glass, which becomes pressure independent above 23 GPa [36]. With increasing pressure, the ductility of GeSe<sub>2</sub> glass is similar to the typical value for metals, for which  $\sigma$  varies between 0.25 and 0.35, while liquids usually have  $\sigma = 0.5$ . This is consistent with the proposed insulator-to-metal transition in glassy GeSe<sub>2</sub> associated with a gradual increase in average coordination number at high pressure, based on *ab initio* molecular dynamics simulations [5]. On depressurization,  $\sigma$  exhibits a small change from  $\sigma = 0.34$  at 9.6 GPa to  $\sigma = 0.28$  at 2 GPa, which is attributed to the irreversible nature of the transition in GeSe<sub>2</sub> glass.

Tkachev *et al.* [6] have argued that amorphous-amorphous transitions need not show a discontinuity with pressure, but more gradual “apparent” second-order-type transitions may exhibit anomalous behavior in Poisson's ratio. The acoustic changes observed in glassy GeSe<sub>2</sub> are consistent with this interpretation. Structural network rigidity, associated with the local atomic bonding constraints of the network, is known to be dominated by the average coordination number of the network forming cation [37] although the effect of pressure has not been formulated to the same extent as freestanding networks [38]. By combining previous spectroscopic [33] and diffraction measurements [15], we show in Fig. 4 that the average Ge coordination number due to local bonding and connectivity has a minimum at  $\sim 3$  GPa, indicating a network rigidity minimum. This network rigidity minimum can also be related to changes in ring size distributions in the glass network. A conversion from edge to corner sharing at low pressure results in larger and more flexible rings, which may be compressed more readily. An increase in coordination reduces the average ring size as the density increases.

Figure 3(d) displays the variations of the elastic moduli with pressure. At 4.6 GPa, there are abrupt increases in the

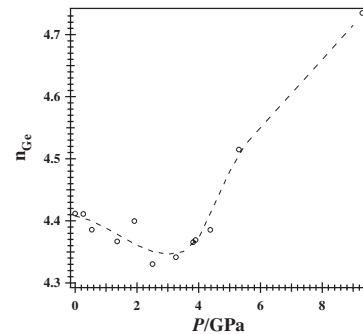


FIG. 4. Variation of local Ge coordination number (including the contribution from edge-shared Ge-Ge tetrahedra). Data were taken from Wang *et al.* [33], which is assumed to be constant beyond 4.3 GPa (a further decrease would make the minimum sharper) and Mei *et al.* [15]. Solid line is a polynomial fit.

bulk and longitudinal moduli, whereas the shear modulus shows a significant slope change. These discontinuities in elastic moduli are indicative of a second-order transition. Below 4 GPa, the shear modulus is essentially constant with  $\partial G/\partial P = 0.134$ ,  $\partial K/\partial P = 7.661$ , and  $\partial L/\partial P = 7.839$ . Above 4 GPa, the derivatives are  $\partial G/\partial P = 2.615$ ,  $\partial K/\partial P = 6.768$ , and  $\partial L/\partial P = 10.255$ . These derivatives are based on least-squares fits to the variation of modulus ( $G$ ,  $K$ , and  $L$ ) with pressure using compressibility data from Mei *et al.* [15] and the initial experimentally determined bulk density  $\rho = 4.204(5) \text{ g cm}^{-3}$ .

In summary, we present a combined ultrasonic interferometry and synchrotron radiation measurement on GeSe<sub>2</sub> glass for precise and simultaneous determination of compressional and shear sound velocities at high pressures. The minimum observed in  $V_S$  but not in  $V_P$  suggests a different densification process in GeSe<sub>2</sub> network glass compared to that of SiO<sub>2</sub>. The main difference is attributed to the conversion of edge- to corner-sharing tetrahedra in GeSe<sub>2</sub> glass up to 3 GPa, which reduces the degree of cross-linking in the network to a minimum despite the continuous increase in density. The type of data from the current measurements provides important information on interpreting changes in the macroscopic properties of glasses with pressure when combined with structural data.

This study was supported by NSF Grants No. EAR-0510501 and No. DMR-0800415 to J.B.P., and DoE/NNSA (No. DEFG5206NA26211) to B.L. The experimental work was performed at X17B2 of the National Synchrotron Light Source (NSLS), supported by the U.S. Department of Energy, Division of Materials Sciences and Division of Chemical Sciences, under Contract No. DE-AC02-98CH10886. This research was partially supported by COMPRES, the Consortium for Materials Properties Research in Earth Sciences under NSF Cooperative Agreement EAR 01-35554.

---

\*Corresponding author.  
sytle.anta@anl.gov

- [1] S. C. Singh, M. A. J. Taylor, and J. P. Montagner, *Science* **287**, 2471 (2000).
- [2] S. M. Antao, I. Jackson, B. Li, J. Kung, J. Chen, I. Hassan, R. C. Liebermann, and J. B. Parise, *Phys. Chem. Miner.* **34**, 345 (2007).
- [3] P. Boolchand, *Phys. Rev. Lett.* **57**, 3233 (1986).
- [4] W. A. Crichton, M. Mezouar, T. Grande, S. Stolen, and A. Grzechnik, *Nature (London)* **414**, 622 (2001).
- [5] M. Durandurdu and D. A. Drabold, *Phys. Rev. B* **65**, 104208 (2002).
- [6] S. N. Tkachev, M. H. Manghnani, and Q. Williams, *Phys. Rev. Lett.* **95**, 057402 (2005).
- [7] M. F. Thorpe, *J. Non-Cryst. Solids* **57**, 355 (1983).
- [8] M. Micoulaut and J. C. Phillips, *Phys. Rev. B* **67**, 104204 (2003).
- [9] P. S. Salmon and I. Petri, *J. Phys. Condens. Matter* **15**, S1509 (2003).
- [10] S. Susman, D. L. Price, K. J. Volin, R. J. Dejus, and D. G. Montague, *J. Non-Cryst. Solids* **106**, 26 (1988).
- [11] S. Susman, K. J. Volin, D. L. Price, M. Grimsditch, J. P. Rino, R. K. Kalia, P. Vashishta, G. Gwanmesia, Y. Wang, and R. C. Liebermann, *Phys. Rev. B* **43**, 1194 (1991).
- [12] P. Vashishta, R. K. Kalia, G. A. Antonio, and I. Ebbsjo, *Phys. Rev. Lett.* **62**, 1651 (1989).
- [13] P. Vashishta, R. K. Kalia, and I. Ebbsjo, *Phys. Rev. B* **39**, 6034 (1989).
- [14] E. Bychkov, C. J. Benmore, and D. L. Price, *Phys. Rev. B* **72**, 172107 (2005).
- [15] Q. Mei, C. J. Benmore, R. T. Hart, E. Bychkov, P. S. Salmon, C. D. Martin, F. M. Michel, S. M. Antao, P. J. Chupas, P. L. Lee, S. D. Shastri, J. B. Parise, K. Leinenweber, S. Amin, and J. L. Yarger, *Phys. Rev. B* **74**, 014203 (2006).
- [16] B. Li, J. Kung, and R. C. Liebermann, *Phys. Earth Planet. Inter.* **143–144**, 559 (2004).
- [17] D. L. Decker, *J. Appl. Phys.* **42**, 3239 (1971).
- [18] B. S. Li, K. Chen, J. Kung, R. C. Liebermann, and D. J. Weidner, *J. Phys. Condens. Matter* **14**, 11 337 (2002).
- [19] J. Kung, B. S. Li, D. J. Weidner, J. Z. Zhang, and R. C. Liebermann, *Earth Planet. Sci. Lett.* **203**, 557 (2002).
- [20] Y. D. Sinelnikov, G. L. Chen, and R. C. Liebermann, *High Press. Res.* **24**, 183 (2004).
- [21] M. Vaughan, J. Chen, L. Li, D. J. Weidner, and B. Li, in *Science and Technology of High Pressure*, edited by M. H. Manghnani, W. J. Nellis, and M. F. Nicol (Universities Press, Hyderabad, India, 2000), p. 1097.
- [22] J. Y. Duquesne and G. Bellessa, *J. Phys. (Paris)* **46**, 445 (1985).
- [23] J. Y. Duquesne and G. Bellessa, *J. Non-Cryst. Solids* **81**, 319 (1986).
- [24] J. Y. Duquesne and G. Bellessa, *Europhys. Lett.* **9**, 453 (1989).
- [25] R. Ota, T. Yamate, N. Soga, and M. Kunugi, *J. Non-Cryst. Solids* **29**, 67 (1978).
- [26] P. W. Bridgman and I. Simon, *J. Appl. Phys.* **24**, 405 (1953).
- [27] M. Grimsditch, *Phys. Rev. Lett.* **52**, 2379 (1984).
- [28] M. Grimsditch, *Phys. Rev. B* **34**, 4372 (1986).
- [29] K. Kondo, S. Lio, and A. Sawaoka, *J. Appl. Phys.* **52**, 2826 (1981).
- [30] A. Polian and M. Grimsditch, *Phys. Rev. B* **47**, 13 979 (1993).
- [31] M. V. N. Prasad, S. Asokan, G. Parthasarathy, S. S. K. Titus, and E. S. R. Gopal, *Phys. Chem. Glasses* **34**, 199 (1993).
- [32] R. Zallen, *Physics of Amorphous Materials* (Wiley, New York, 1984).
- [33] F. Wang, S. Mamedov, P. Boolchand, B. Goodman, and M. Chandrasekhar, *Phys. Rev. B* **71**, 174201 (2005).
- [34] P. S. Salmon, R. A. Martin, P. E. Mason, and G. J. Cuello, *Nature (London)* **435**, 75 (2005).
- [35] X. W. Feng, W. J. Bresser, and P. Boolchand, *Phys. Rev. Lett.* **78**, 4422 (1997).
- [36] C. S. Zha, R. J. Hemley, H. K. Mao, T. S. Duffy, and C. Meade, *Phys. Rev. B* **50**, 13 105 (1994).
- [37] S. S. Yun, H. Li, R. L. Cappelletti, R. N.ENZWEILER, and P. Boolchand, *Phys. Rev. B* **39**, 8702 (1989).
- [38] H. Yan, A. R. Day, and M. F. Thorpe, *Phys. Rev. B* **38**, 6876 (1988).